PHYSICAL REVIEW B VOLUME 51, NUMBER 15 15 APRIL 1995-I

Small-signal ac response of an electron gas under a strong dc bias

Z. Q. Zou
Shanghai Institute of Metallurgy, Chinese Academy of Sciences, 865 Changning Road, Shanghai 200050, China

X. L. Lei
China Center of Advanced Science and Technology (World Laboratory), P.O. Box 8730, Beijing 100080, China and Shanghai Institute of Metallurgy, Chinese Academy of Sciences, 865 Changning Road, Shanghai 200050, China

(Received 19 August 1994; revised manuscript received 20 December 1994)

We analyze the small-signal ac response of an electron gas with or without a dc bias, including contributions due to plasma modes and electron temperature oscillations. It is pointed that under a strong dc bias the prominent plasma-induced structure showing up in the 0-K memory function is greatly suppressed by the rise of the electron temperature in a realistic semiconductor, in contrast with the earlier result. Oscillation of the electron temperature also plays an important role in the ac response in a parallel configuration at low frequency under a strong dc bias.

The high-frequency ac response of semiconductor materials has been the subject of many theoretical studies in the literature.[1–7] When only a weak-signal ac electric field was applied, a good understanding of the dynamic conductivity has been achieved for a two-dimensional electron gas, where significant contributions from plasma excitations to the real and imaginary parts of the memory function show up at low lattice temperatures.[3–5] The effect of the intercarrier Coulomb interactions on the high-frequency response in a three-dimensional bulk material, on the other hand, is relatively less clear. The situation becomes more complicated when a strong dc bias field is simultaneously applied. The balance-equation theory developed by Lei and Ting[8] provides a very convenient tool for investigating the effect of a strong dc electric field on the ac response of an electron system when the role of the electron collective modes is included. Dynamic conductivity under the influence of a dc bias was systematically discussed by Cai *et al.*[9] on the basis of the balance-equation approach, with an emphasis on the large ac-signal response. A comprehensive analysis concerning small-signal conductivity has also been given by Lei and Horing.[10] Recently Ma and Shung[11] carried out a detailed calculation of the high-frequency small-signal conductivity limited by the impurity scattering in n-doped bulk GaAs, and found that the optical reflection and absorption coefficients of the system could experience drastic changes at the frequency ω around the plasma frequency ω_p due to the prominent structure in the memory function at $\omega \sim \omega_p$, even when a strong bias electric field is applied such that the dc drift velocity v_d is as large as the Fermi velocity v_F of the system. This result, however, relies on their assumption that electrons stay as cool as the lattice, which is considered to be at zero temperature, even when a strong bias dc current (with drift velocity $v_d \sim v_F$) flows in the system. Such a model, which requires an infinitely strong mechanism to dissipate electron energy while it contributes nothing to the frictional forces, is far from a true GaAs system. The purpose of this paper is to take account of the realistic energy-dissipation mechanisms (phonon scatterings) in bulk GaAs, and to calculate the small-signal ac response of the system under the influence of dc biases of various strengths. We find that the electron temperature at bias $v_d \sim v_F$, determined by the energy-balance equation, is so high (even at zero lattice temperature) that the previous (zero electron temperature) huge hump around $\omega \sim \omega_p$ in the imaginary part of the memory function is greatly suppressed, leading to a relatively structureless high-frequency resistivity $\rho(\omega, v_d)$, in contrast to $\rho(\omega, 0)$ at zero dc bias. Furthermore, unlike the case without a dc bias, under the influence of a nonzero dc bias a small change of the electric field (in the bias-field direction) gives rise to a small change of the electron temperature in the linear order, resulting in an additional contribution to the small-signal ac parallel resisitivity, thus a different result at low frequency from that evaluated based on the formula pertinent to the case without a dc bias.

We consider a small-amplitude ac-signal electric field $2\mathbf{E}_1\cos\omega t$ applied to an isotropic system together with a constant dc bias field $\mathbf{E}_0$:

$$\mathbf{E}(t)=\mathbf{E}_0+\mathbf{E}_1 e^{-i\omega t}+\mathbf{E}_1 e^{i\omega t} . \quad (1)$$

It is obvious that after a transient process the system will reach an oscillatory steady state in which the center of mass moves at a constant drift velocity $\mathbf{v}_d$ and oscillates with a small amplitude at the single driving frequency ω,

$$\mathbf{v}(t)=\mathbf{v}_d+\mathbf{v}_1 e^{-i\omega t}+\mathbf{v}_1^* e^{i\omega t} , \quad (2)$$

and that the electron temperature $T_e(t)$ will also experience a small-amplitude harmonic oscillation about a constant value T_e,

$$T_e(t)=T_e+T_1 e^{-i\omega t}+T_1^* e^{i\omega t} . \quad (3)$$

These, to leading order in the small quantities, provide the frictional force $\mathbf{f}=\mathbf{f}_i+\mathbf{f}_p$ (due to impurity and phonon scatterings) and the energy transfer rate w (due to phonon scattering) with the following expressions:

 ©1995 The American Physical Society

$$\mathbf{f}=\mathbf{f}_0+\mathbf{f}_0^{(1)}(T_1e^{-i\omega t}+T_1^*e^{i\omega t})+(\mathbf{f}_1e^{-i\omega t}+\mathbf{f}_1^*e^{i\omega t}) , \quad (4)$$

$$w=w_0+w_0^{(1)}(T_1e^{-i\omega t}+T_1^*e^{i\omega t})+(w_1e^{-i\omega t}+w_1^*e^{i\omega t}) . \quad (5)$$

Here $\mathbf{f}_0=\mathbf{f}_0(v_d,T_e)$ and $w_0=w_0(v_d,T_e)$ are the well-known force- and energy-transfer rate expressions in the dc steady state,[8] with drift velocity v_d and electron temperature T_e; $\mathbf{f}_0^{(1)}\equiv\partial\mathbf{f}_0(v_d,T_e)/\partial T_e$ and $w_0^{(1)}\equiv\partial w_0(v_d,T_e)/\partial T_e$. $\mathbf{f}_1=\mathbf{f}_1(\omega,v_d,T_e)$ and $w_1=w_1(\omega,v_d,T_e)$ are frequency-dependent linear-order small quantities related to the memory effect. Their zero-frequency values are just $\mathbf{f}_1(0,v_d,T_e)=\mathbf{v}_1\cdot\partial\mathbf{f}_0(v_d,T_e)/\partial\mathbf{v}_d$ and $w_1(0,v_d,T_e)=\mathbf{v}_1\cdot\partial w_0(v_d,T_e)/\partial\mathbf{v}_d$. For their full expressions please refer to Refs. 9 and 10.

The force- and energy-balance equations[8,10] can then be written up to linear order in the small-amplitude ac quantities. For zeroth order we have exactly the same balance equations as those in the dc steady state:

$$ne\mathbf{E}_0+\mathbf{f}_0=\mathbf{0} , \quad (6)$$

$$\mathbf{v}_d\cdot\mathbf{f}_0+w_0=0 , \quad (7)$$

which determine the dc drift velocity $\mathbf{v}_d$ and the electron temperature T_e for a given bias field $\mathbf{E}_0$. The linear-order ac balance equations are[9,10]

$$-i\omega nm\mathbf{v}_1=ne\mathbf{E}_1+\mathbf{f}_0^{(1)}T_1+\mathbf{f}_1 \quad (8)$$

and

$$i\omega C_eT_1=\mathbf{v}_1\cdot\mathbf{f}_0+(\mathbf{v}_d\cdot\mathbf{f}_0^{(1)}+w_0^{(1)})T_1+\mathbf{v}_d\cdot\mathbf{f}_1+w_1 , \quad (9)$$

where C_e is the specific heat of the electron system at the bias electron temperature T_e. From Eqs. (8) and (9) the ac quantities $\mathbf{v}_1$ and T_1 can be determined for a given ac-signal field $\mathbf{E}_1$.

Let $\mathbf{E}_0$ be along the z direction and $\mathbf{E}_1$ in the x-z plane, $\mathbf{E}_1=E_{1x}\hat{x}+E_{1x}\hat{z}$. For an isotropic system, $\mathbf{v}_d$ and $\mathbf{f}_0$ are along the z direction and $\mathbf{v}_1$ and $\mathbf{f}_1$ are in the x-z plane. We can write $\mathbf{v}_1=v_{1x}\hat{x}+v_{1z}\hat{z}$, and

$$\mathbf{f}_1=inmv_{1x}M_\perp(\omega,v_d)\hat{x}+inmv_{1z}M_\parallel(\omega,v_d)\hat{z} , \quad (10)$$

where $M_{\perp(\parallel)}(\omega,v_d)$ are the momentum-related memory functions at a bias drift velocity v_d, which consists of contributions from impurities $M_{\perp(\parallel)}^{(i)}(\omega,v_d)$, and from phonons $M_{\perp(\parallel)}^{(p)}(\omega,v_d)$. Their expressions were given in Refs. 9, 10, and 12. The momentum-related memory function will simply be called the memory function. Furthermore, w_1 is independent of v_{1x}, and can be written in the form

$$w_1=inmv_dv_{1z}N(\omega,v_d) , \quad (11)$$

where

$$N(\omega,v_d)=\frac{1}{nm\omega v_d}\sum_{\mathbf{q},\lambda}q_z\Omega_{\mathbf{q}\lambda}|M(\mathbf{q},\lambda)|^2 \times[\Gamma(\mathbf{q},\lambda,q_zv_d)-\Gamma(\mathbf{q},\lambda,q_zv_d+\omega)] \quad (12)$$

is the energy-related memory function. In Eq. (12), the imaginary and real parts of the correlation function $\Gamma(\mathbf{q},\lambda,\omega)$ are expressed as

$$\Gamma_2(\mathbf{q},\lambda,\omega)=\Pi_2(\mathbf{q},\omega+\Omega_{\mathbf{q}\lambda})\left[n\left[\frac{\Omega_{\mathbf{q}\lambda}}{T}\right]-n\left[\frac{\Omega_{\mathbf{q}\lambda}+\omega}{T_e}\right]\right]-\Pi_2(\mathbf{q},\omega-\Omega_{\mathbf{q}\lambda})\left[n\left[\frac{\Omega_{\mathbf{q}\lambda}}{T}\right]-n\left[\frac{\Omega_{\mathbf{q}\lambda}-\omega}{T_e}\right]\right] \quad (13)$$

and

$$\Gamma_1(\mathbf{q},\lambda,\omega)=[\Pi_1(\mathbf{q},\omega+\Omega_{\mathbf{q}\lambda})-\Pi_1(\mathbf{q},\omega-\Omega_{\mathbf{q}\lambda})]n\left[\frac{\Omega_{\mathbf{q}\lambda}}{T}\right]+\frac{1}{\pi}\int_{-\infty}^{+\infty}d\omega_1\Pi_2(\mathbf{q},\omega_1)n\left[\frac{\omega_1}{T_e}\right]\left[\frac{1}{\omega_1+\omega-\Omega_{\mathbf{q}\lambda}}-\frac{1}{\omega_1-\omega-\Omega_{\mathbf{q}\lambda}}\right] . \quad (14)$$

Here $n(x)=1/[\exp(x)-1]$ is the Bose function, $\Pi_1(\mathbf{q},\omega)$ and $\Pi_2(\mathbf{q},\omega)$, respectively, are the real and imaginary parts of the electron-density correlation function.

With these, we find that the x component of Eq. (8) determines v_{1x} proportional to E_{1x}, leading to a perpendicular complex small-signal resistivity or conductivity

$$\rho_\perp(\omega,v_d)\equiv1/\sigma_\perp(\omega,v_d) =\frac{E_{1x}}{nev_{1x}}=-i\frac{m}{ne^2}[\omega+M_\perp(\omega,v_d)] , \quad (15)$$

as given in Ref. 11. On the other hand, the z components of Eq. (8) and Eq. (9) determine v_{1z} proportional to E_{1z}, yielding a parallel complex small-signal resistivity or conductivity, different from that of Ref. 11:

$$\rho_\parallel(\omega,v_d)\equiv1/\sigma_\parallel(\omega,v_d) =\frac{E_{1z}}{nev_{1z}}=-i\frac{m}{ne^2}[\omega+M_\parallel(\omega,v_d)+D(\omega)] , \quad (16)$$

where

$$D(\omega)=-\frac{v_df_0^{(1)}[M_\parallel(\omega,v_d)+N(\omega,v_d)+i\tau_0^{-1}]}{v_df_0^{(1)}+w_0^{(1)}-i\omega C_e} , \quad (17)$$

with $\tau_0^{-1}=-f_0/nmv_d$ being the effective inverse scattering time related to the dc nonlinear resistivity at the bias field.

In the absence of a dc bias $\mathbf{E}_0=0$, the zero-order equations (6) and (7) yield $\mathbf{v}_d=0$ and $T_e=T$. We thus have $D(\omega)=0$ and $M_\parallel(\omega,0)=M_\perp(\omega,0)=M(\omega)$. The small-signal conductivity in the zero dc bias is direction in-

dependent, and is given by Eq. (15). In the presence of a finite dc bias, $\rho_{\parallel}(\omega,v_d)$ differs from $\rho_{\perp}(\omega,v_d)$ not only due to $M_{\parallel}(\omega,v_d)$ differing from $M_{\perp}(\omega,v_d)$, but also due to the additional term $D(\omega)$ in the parallel case. This is because a small ac current parallel to the dc bias field induces an energy (thus an electron temperature) change in the linear order, while a small perpendicular ac current can induce the energy (temperature) change only in higher order. A random current fluctuation is not able to induce such a change no matter whether it is parallel or perpendicular to the bias dc field. Therefore, the noise conductivity at a nonzero dc bias is always given by the simple formula

$$\sigma_{n\perp(\parallel)}(\omega,v_d)=i\frac{ne^2}{m}\frac{1}{\omega+M_{\perp(\parallel)}(\omega,v_d)}\ , \tag{18}$$

for both parallel and perpendicular directions. Equation (18) was used in discussing the thermal noise temperature and diffusion under a strong dc electric field.[12,13]

As an example, we consider exactly the same system as that discussed in Ref. 11: n-doped GaAs at lattice temperature $T=0$ K, with a doping concentration $n_i=1.4\times10^{16}$ cm^{-3} and a conduction electron density $n=n_i$. We take the electron effective mass $m=0.067m_e$ (m_e stands for the free-electron mass); static dielectric constant $\kappa=12.9$, optic dielectric constant $\kappa_\infty=10.9$, leading to a zero-temperature Fermi level $\varepsilon_F=3.14$ meV (counted from the conduction-band bottom) or Fermi temperature $T_F=36.4$ K; Fermi velocity $v_F=1.28\times10^5$ m/s and plasma frequency $\omega_p=7.79\times10^{12}$/s. Scatterings from charged impurities, acoustic phonons (through deformation potential and piezoelectric couplings with electrons), and longitudinal-optical (LO) phonons (through Fröhlich couplings with electrons) are taken into account. The other relevant material and electron-phonon-coupling parameters are chosen as in Refs. 11 and 14: acoustic deformation potential $\Xi=8.6$ eV,

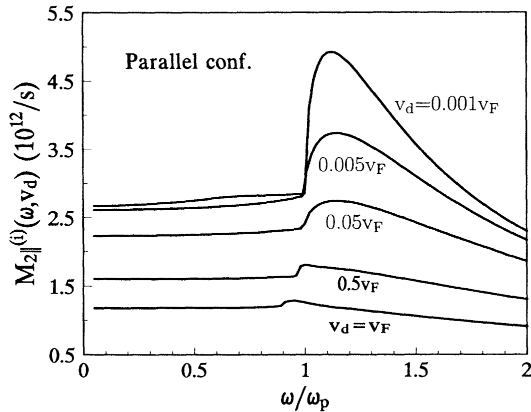

FIG. 1. Imaginary part of the impurity-induced memory function in the parallel configuration, $M_{2\parallel}^{(i)}(\omega,v_d)$, is shown as a function of the reduced frequency ω/ω_p at bias drift velocities $v_d=0.001v_F$, $0.005v_F$, $0.05v_F$, $0.5v_F$, and $1.0v_F$, corresponding to electron temperatures $T_e=2.6$, 22, 46, 86, and 113 K, respectively.

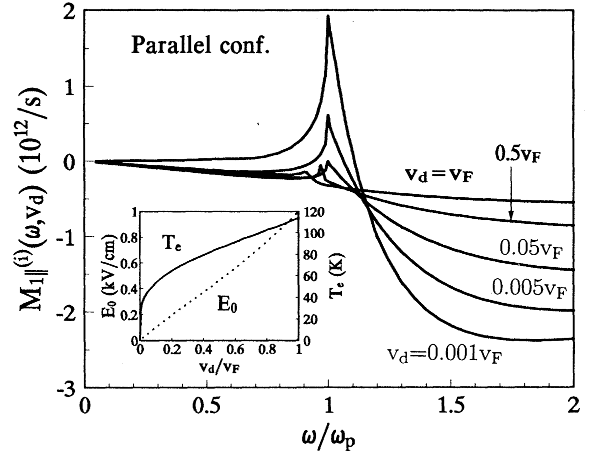

FIG. 2. Real part of the impurity-induced memory function in the parallel configuration, $M_{1\parallel}^{(i)}(\omega,v_d)$, is shown as a function of the reduced frequency ω/ω_p at bias drift velocities $v_d=0.001v_F$, $0.005v_F$, $0.05v_F$, $0.5v_F$, and $1.0v_F$, corresponding to electron temperatures $T_e=2.6$, 22, 46, 86, and 113 K, respectively. The inset indicates the bias electric field E_0 and the electron temperature T_e against the bias drift velocity, as determined from Eqs. (6) and (7).

piezoelectric constant $e_{14}=1.41\times10^9$ V/m, LO-phonon frequency $\Omega_{\rm LO}=5.38\times10^{13}$/s, longitudinal sound velocity $v_{\rm sl}=5.29\times10^3$m/s, transverse sound velocity $v_{\rm st}=2.48\times10^3$ m/s, and mass density $d=5.31$ g/cm^3.

In the calculation of the momentum- and energy-related memory functions, the random-phase approximation (Lindhard dielectric function) is used to take account of effects of the electron dynamic screening and contributions from plasma excitations. The calculated imaginary part of the impurity-induced memory functions in the parallel configuration $M_{2\parallel}^{(i)}(\omega,v_d)$ is shown in Fig. 1 as a function of the reduced frequency ω/ω_p. In the case of zero or very small dc bias, when the electron temperature T_e remains much lower than T_F, e.g., $v_d=0.001$ v_F ($T_e=2.6$ K), $M_{2\parallel}^{(i)}(\omega,v_d)$ has a remarkable enhancement (about 75% over its value immediately before the enhancement) starting from $\omega=\omega_p$, and exhibits a huge hump in the frequency range between ω_p and $1.7\omega_p$ before it decreases at high frequency. This is almost the same as the $v_d=0v_F$ result obtained by Ma and Shung.[11] However, with increasing dc bias velocity, the electron temperature increases quickly, and the height of the plasmon-induced hump is greatly suppressed, together with a small shift of its position toward lower frequency. At a bias of $v_d=0.5v_F$ ($T_e=86$ K) the largest enhancement is less than 10%. These results are in strong contrast with those of Ref. 11. Correspondingly, the sharp peaks in the real part of the memory function, showing up at zero dc bias, are greatly weakened with increasing the bias drift velocity, and almost disappear when $v_d>0.5v_F$ (see Fig. 2). The imaginary and real parts of $M_{\perp}^{(i)}(\omega,v_d)$ also exhibit similar behavior.

To estimate the effect of the electron-temperature oscil-

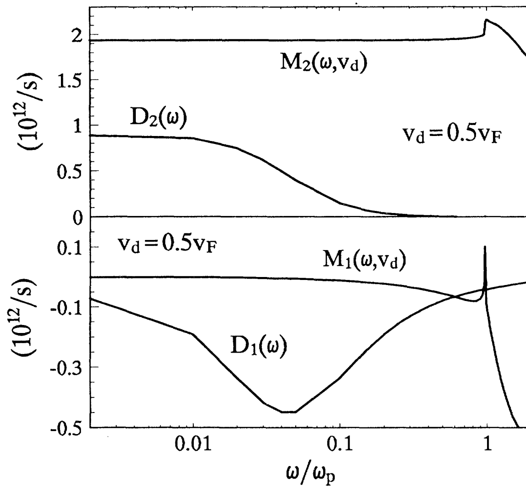

FIG. 3. Real and imaginary parts of $D(\omega)$, and the memory function in the parallel configuration, are shown as functions of reduced frequency ω/ω_p in the case of bias drift velocity $v_d = 0.5v_F$ ($T_e = 86$ K).

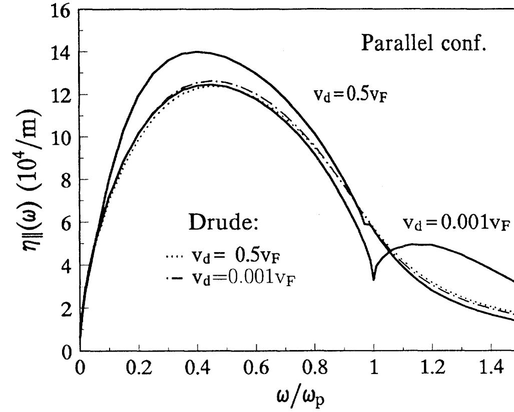

FIG. 4. Absorption coefficient in the parallel configuration, $\eta_\parallel(\omega)$, is shown as a function of the reduced frequency ω/ω_p for dc biases $v_d = 0.001v_F$ and $0.5v_F$, together with corresponding Drude forms (dashed and chain curves).

lation on the parallel complex resistivity, we need to calculate $D(\omega)$ and compare it with $M_\parallel(\omega, v_d)$. Obviously, in the zero-frequency limit $\omega \to 0$, its real part $D_1(\omega)$ approaches zero, and its imaginary part $D_2(\omega)$ approaches a finite value. Furthermore, at small dc biases both $D_1(\omega)$ and $D_2(\omega)$ are negligibly small and $\rho_\parallel$ and $\rho_\perp$ share essentially the same expression (the difference between $M_\parallel$ and $M_\perp$ also becomes very small at small dc bias). In a strong dc bias, however, the $D(\omega)$-related contribution is important at low frequency, as is seen from Fig. 3, where we show $D_1(\omega)$ and $D_2(\omega)$ as functions of frequency in the case of $v_d = 0.5v_F$, together with the real and imaginary parts of the memory function, $M_{1\parallel}(\omega, v_d)$ and $M_{2\parallel}(\omega, v_d)$. Both $D_1(\omega)$ and $D_2(\omega)$ approach zero at high frequency ($\omega > 0.2\omega_p$), reflecting the fact that the electron temperature cannot follow a very rapid oscillation of the driving field. This should be compared with the momentum-related memory functions $M_{1\parallel}(\omega, v_d)$ and $M_{2\parallel}(\omega, v_d)$, which approach zero only when $\omega \gg 2\omega_p$. This indicates that the energy relaxation time is more than ten times longer than the momentum relaxation time.

The reflection and absorption coefficients are easily obtained from the results of $M_\parallel(\omega, v_d)$ and $D(\omega)$. Figure 4 shows the absorption coefficient in the parallel configuration, $\eta_\parallel(\omega)$, as a function of photon frequency for two dc biases, $v_d = 0.001v_F$ and $0.5v_F$, together with corresponding Drude forms (dashed and chain curves). In the case of $v_d = 0.001v_F$ the result is similar to that reported in Ref. 11: $\eta_\parallel(\omega)$ exhibits a marked dip at $\omega = \omega_p$ before forming a bulge at the higher frequency. On the other hand, in the case of $v_d = 0.5v_F$, the absorption coefficient shows an almost smooth change with frequency (except a small kink at ω_p), somewhat similar to the behavior of the Drude form.

The author thanks the Chinese National Natural Science Foundation and the Chinese National and Shanghai Municipal Commissions of Science and Technology for support of this work.

[1]A. Ron and N. Tzoar, Phys. Rev. **131**, 1943 (1963).
[2]W. Götze, and P. Wöfle, Phys. Rev. B **6**, 1226 (1973).
[3]T. A. Kennedy, R. J. Wagner, B. D. McCombe, and D. C. Tsui, Phys. Rev. Lett. **35**, 1109 (1975).
[4]C. S. Ting, A. K. Ganguly, and W. Y. Lai, Phys. Rev. B **24**, 3371 (1981).
[5]X. L. Lei and J. Q. Zhang, J. Phys. C **19**, L73 (1986); X. L. Lei and N. J. M. Horing, Phys. Rev. B **33**, 2912 (1986).
[6]P. A. Lebwohl, J. Appl. Phys. **44**, 1744 (1973).
[7]P. Das and D. K. Ferry, Solid State Electron. **19**, 851 (1976).
[8]X. L. Lei and C. S. Ting, Phys. Rev. B **30**, 4809 (1984); **32**, 1112 (1985).
[9]W. Cai, P. Hu, T. F. Zheng, B. Yudanin, and M. Lax, Phys. Rev. B **40**, 7671 (1989).
[10]X. L. Lei and N. J. M. Horing, Int. J. Mod. Phys. **6**, 805 (1992).
[11]S.-K. Ma and K.W.-K. Shung, Phys. Rev. B **48**, 10 751 (1993).
[12]X. L. Lei and N. J. M. Horing, Phys. Rev. B **36**, 4238 (1987).
[13]P. Hu and C. S. Ting, Phys. Rev. B **35**, 4162 (1987).
[14]X. L. Lei, J. L. Birman, and C. S. Ting, J. Appl. Phys. **58**, 2270 (1985).